Inorganica Chimica Acta 394 (2013) 757–764

Contents lists available at SciVerse ScienceDirect

Inorganica Chimica Acta

journal homepage: www.elsevier.com/locate/ica

Synthesis, characterization, X-ray structure and spectroscopic study of platinum(II) complexes with tridentate diazene ligands having O,N,S donor set

Suvra Acharya [a], Ambica Kejriwal [a], Achintesh Narayan Biswas [b], Purak Das [a], Debatra Narayan Neogi [a], Pinaki Bandyopadhyay [a,*]

[a] Department of Chemistry, University of North Bengal, Raja Rammohunpur, Siliguri 734013, India
[b] Department of Chemistry, Siliguri College, Siliguri 734001, India

ARTICLE INFO

Article history:
Received 25 May 2012
Received in revised form 28 September 2012
Accepted 28 September 2012
Available online 9 October 2012

Keywords:
Platinum
Diazene
O,N,S donors
TD-DFT

ABSTRACT

At room temperature, 2-hydroxy-1-(2′-alkylthiophenylazo)naphthalenes and 1-hydroxy-2-(2′-alkylthiophenylazo)napthalenes (HL) slowly react with di-μ-chloro-bis(η^3-2-methylallyl)platinum(II) in chloroform and afford complexes of the type [Pt^{II}(L)Cl]. Potassium tetrachloroplatinate also reacts with the HL group of ligands in acetonitrile medium under reflux condition and produces complexes of the type [Pt^{II}(L)Cl]. All the platinum complexes [Pt^{II}(L)Cl] have been successfully isolated in pure form and characterized by spectroscopic techniques. The solid state structures of [$Pt^{II}(L^3)$Cl] (**3**) and [$Pt^{II}(L^9)$Cl] (**9**) have been determined by single crystal X-ray diffraction. The crystal structures have revealed that diazene ligands bind to the metal ion as monoanionic terdentate O,N,S donors and the fourth coordination position is occupied by a halide ion. All the platinum(II) complexes absorb strongly in the ultraviolet and visible region. The TD-DFT (time-dependent density functional theory) calculation has been carried out for better understanding of the electronic structure of platinum(II) complexes and the nature of spectral transitions. The low energy absorptions are attributed to intraligand charge transfer transitions having admixtures of metal-to-ligand charge-transfer transitions whereas the high energy absorptions are due to ILCT and LLCT transitions. The reactivity of [Pt^{II}(L)Cl] with iodine and methyl iodide has been studied.

1. Introduction

The serendipitous discovery of the antiproliferative and cytotoxic activities of cisplatin [1–3] has generated tremendous amount of interest on the coordination chemistry of platinum(II) [4–11]. However, due to the toxic side effects of cisplatin [12], efforts have been devoted to the development of alternative anticancer agents based on platinum(II) [13–17]. An improved strategy developed in this regard relies on the design of complexes containing a Pt(II)–S bond [13]. This strategy is initiated primarily because of the detoxicant properties of sulfur containing ligands and the lability of Pt–S bond in presence of other nucleophiles [18]. A number of platinum(II) complexes with bidentate N,S ligands have been shown to be potential anticancer drugs [19]. However, the use of tridentate ligands in generation of antiproliferative metal complexes is relatively sparse. A new Au(III) complex derived from tridentate 2-(phenylazo)pyridine in 2007, has been tested in vitro in a number of tumor cell lines and showed promising cytotoxic activity [20].

On the other hand, the reactivity of platinum(II) with aryldiazenes [21–25] added a new dimension to metal mediated intramolecular C(aryl)–H bond activation [26]. Since then, platinum complexes with diazene ligands having N,S [27], N,N [23,24,28], C,N,O [25] and C,N,S [21,22] coordination spheres have been reported in the literature.

Here, we have examined the reactivity of platinum(II) towards tridentate ligands (HL^1–HL^{10}) with O(naphtholato),N(diazene),S(thioether) donor set. The isolation and structural characterization of the resulting platinum(II) complexes have been described. The reactivity of platinum(II) complexes with iodine and methyl iodide has been studied. The isolation and characterization of the products have been done.

2. Experimental

2.1. Materials

Commercial potassium tetrachloroplatinate $K_2[PtCl_4]$ was purchased from Arora Matthey Ltd., Kolkata, India. 1-Chloro-2-methyl prop-2-ene (Merck, Germany), 2-aminothiophenol (Merck, Germany), 1-naphthol, 2-naphthol (R. Merck, India), sodium acetate, silica gel, methyl iodide, ethyl bromide, *n*-propyl bromide, butyl

* Corresponding author. Tel.: +91 353 2776381; fax: +91 353 2699001.
E-mail address: pbchem@rediffmail.com (P. Bandyopadhyay).

0020-1693/$ - see front matter © 2012 Elsevier B.V. All rights reserved.
http://dx.doi.org/10.1016/j.ica.2012.09.041

bromide and benzyl chloride (SD Fine Chemicals, India) were used without further purification. All solvents were purified according to standard procedures. Solid iodine (SM, India) was purified by sublimation. Complex di-μ-chloro-bis(η^3-2-methylallyl)platinum(II), $[Pt(allyl)Cl]_2$, was synthesized following reported method [29].

2.2. Synthesis of the ligands

2-Hydroxy-1-(2′-alkylthiophenylazo)naphthalenes (HL^1–HL^5) and 1-hydroxy-2-(2′-alkylthiophenylazo)naphthalenes (HL^6–HL^{10}) were prepared following reported procedure using 2-naphthol and 1-naphthol, respectively [30].

2.3. Synthesis of platinum(II) complexes

2.3.1. Isolation of $[Pt(L^1)Cl]$ (**1**)

2.3.1.1. Procedure (1). HL^1 (0.02 g, 0.07 mmol) was dissolved in chloroform (10 mL). Then the orange yellow ligand solution was added dropwise to a solution of $[Pt(allyl)Cl]_2$ complex (0.02 g, 0.035 mmol) in chloroform (10 mL) and stirred at room temperature. The yellow color of mixture turned into pink very slowly and the stirring of the mixture was continued for 24 h at room temperature. The solvent was then evaporated to give a solid mass. The solid mass was dissolved in dichloromethane and subjected to purification by thin layer chromatography using ethyl acetate as eluant. A pink band was separated and extracted with methanol (yield: 0.026 g, 0.05 mmol, 74%).

2.3.1.2. Procedure (2). The ligand HL^1 (0.07 g, 0.24 mmol) was dissolved in 100 mL acetonitrile. To this was added an aqueous solution of $K_2[PtCl_4]$ (0.1 g, 0.24 mmol) and the mixture was refluxed on a steam bath for 3 h. During the period the orange color of the mixture slowly became reddish-orange. The reaction mixture was then cooled and filtered. It was left undisturbed for slow evaporation. After three days dark crystalline products, deposited in the reaction vessel, were collected by filtration and washed thoroughly with diethyl ether and finally air-dried in a vaccum dessicator (Yield: 85%). *Anal.* Calc. for $C_{17}H_{13}N_2OSClPt$: C, 39; H, 2.5; N, 5.3. Found: C, 38.3; H, 2.0; N, 4.9%. IR (KBr; ν/cm^{-1}): 1437 (–N=N–). UV–Vis (CH_2Cl_2), λ/nm ($\varepsilon/dm^3\,mol^{-1}\,cm^{-1}$): 401 (4900), 522 (5000), 553 (7000). ^{1}H NMR in $CDCl_3$ (ppm): 3.01 (s, 3H, $-SCH_3$), 7.21–7.84 (8H), 8.48 (d, 1H, J = 8.4 Hz), 8.86 (d, 1H, J = 8.2 Hz). MS: m/z 523 $[M]^+$.

2.3.2. Isolation of $[Pt(L^2)Cl]$ (**2**)

$[Pt(L^2)Cl]$ was made following the same procedure of complex **1**. The following yield is based on HL^2 (0.025 g, 0.07 mmol) and $[Pt(allyl)Cl]_2$ (0.02 g, 0.035 mmol) (Yield: 0.029 g, 0.054 mmol, 77%). *Anal.* Calc. for $C_{18}H_{15}N_2OSClPt$: C, 40.0; H, 2.8; N, 5.2. Found: C, 39.4; H, 2.71; N, 4.9%. IR (KBr; ν/cm^{-1}): 1436 (–N=N–). UV–Vis (CH_2Cl_2), λ/nm ($\varepsilon/dm^3\,mol^{-1}\,cm^{-1}$): 401 (5900), 522 (5400), 554 (7300). ^{1}H NMR in $CDCl_3$ (ppm): 3.51 (m, 2H, $-SCH_2$), 1.24 (t, 3H, $-CH_3$), 7.18 (d, 1H, J = 9.2 Hz), 7.42–7.55 (m, 3H), 7.61 (d, 1H, J = 8.0 Hz), 7.68–7.77 (m, 3H), 8.50 (d, 1H, J = 8.4 Hz), 8.86 (d, 1H, J = 8.0 Hz). MS: m/z 537 $[M]^+$.

2.3.3. Isolation of $[Pt(L^3)Cl]$ (**3**)

$[Pt(L^3)Cl]$ (**3**) was made following the same procedure of complex **1**. The amount of HL^3 and $[Pt(allyl)Cl]_2$ used were (0.023 g, 0.07 mmol) and (0.020 g, 0.035 mmol), respectively (Yield: 0.018 g, 0.055 mmol, 79%). *Anal.* Calc. for $C_{19}H_{17}N_2OSClPt$: C, 41.3; H, 3.1; N, 5.1. Found: C, 40.9; H, 2.71; N, 4.9%. IR (KBr; ν/cm^{-1}): 1438 (–N=N–). UV–Vis (CH_2Cl_2), λ/nm ($\varepsilon/dm^3\,mol^{-1}\,cm^{-1}$): 400 (6300), 522 (6500), 554 (9200). ^{1}H NMR in $CDCl_3$ (ppm): 3.49 (m, 2H, $-SCH_2$), 1.26 (m, 2H, $-CH_2$), 1.08 (t, 3H, $-CH_3$), 7.16 (m, 1H), 7.39–7.49 (m, 5H), 7.69–7.80 (m, 2H), 8.07 (d, 1H, J = 9.6 Hz), 8.63 (d, 1H, J = 7.6 Hz). MS: m/z 551 $[M]^+$.

2.3.4. Isolation of $[Pt(L^4)Cl]$ (**4**)

$[Pt(L^4)Cl]$ (**4**) was made following the same procedure of complex **1**. The following yield is based on HL^4 (0.024 g, 0.07 mmol) and $[Pt(allyl)Cl]_2$ complex (0.02 g, 0.035 mmol) (Yield: 0.031 g, 0.054 mmol, 77%). *Anal.* Calc. for $C_{20}H_{19}N_2OSClPt$: C, 42.4; H, 3.4; N, 5. Found: C, 41.9; H, 3.0; N, 4.7%. IR (KBr; ν/cm^{-1}): 1437 (–N=N–). UV–Vis (CH_2Cl_2), λ/nm ($\varepsilon/dm^3\,mol^{-1}\,cm^{-1}$): 305 (4600), 401 (6700), 523 (6800), 554 (9600). ^{1}H NMR in $CDCl_3$ (ppm): 3.50 (m, 2H, $-SCH_2$), 1.63 (m, 2H, $-CH_2$), 1.24 (m, 2H, $-CH_2$), 0.88 (m, 3H, $-CH_3$), 7.18 (br, 1H), 7.32–7.49 (m, 3H), 7.57–7.61 (m, 2H), 7.68–7.75 (m, 2H), 8.06 (d, 1H, J = 9.2 Hz), 8.60 (d, 1H, J = 8.8 Hz). MS: m/z 565 $[M]^+$.

2.3.5. Isolation of $[Pt(L^5)Cl]$ (**5**)

$[Pt(L^5)Cl]$ (**5**) was made following the same procedure of complex **1**. The following yield is based on HL^5 (0.026 g, 0.07 mmol) and $[Pt(allyl)Cl]_2$ complex (0.02 g, 0.035 mmol) (Yield: 0.03 g, 0.05 mmol, 70%). *Anal.* Calc. for $C_{23}H_{17}N_2OSClPt$: C, 46; H, 2.8; N, 4.7. Found: C, 45.8; H, 2.71; N, 4.2%. IR (KBr; ν/cm^{-1}): 1436 (–N=N–). UV–Vis (CH_2Cl_2), λ/nm ($\varepsilon/dm^3\,mol^{-1}\,cm^{-1}$): 310 (5600), 402 (7400), 523(7500), 555 (10400). ^{1}H NMR in $CDCl_3$ (ppm): 3.48 (m, 2H, $-SCH_2$), 7.18–7.34 (m, 6H), 7.39–7.46 (m, 4H), 7.73–7.75 (br, 2H), 8.06 (d, 1H, 9.2 Hz), 8.57 (d, 1H, 8.4 Hz). MS: m/z 599 $[M]^+$, 564 $[M-Cl]^+$.

2.3.6. Isolation of $[Pt(L^6)Cl]$ (**6**)

A pink colored solution of HL^6 (0.009 g, 0.03 mmol) in chloroform (10 mL) was slowly added dropwise to a solution of $[Pt(allyl)Cl]_2$ (0.009 g, 0.015 mmol) in chloroform (10 mL) and stirred at room temperature. The pink color of the reaction mixture immediately turned into violet and stirring of the mixture was continued for 3 h. The solvent was then evaporated to give a solid mass. The solid mass was then dissolved in dichloromethane and subjected to purification by TLC, using ethyl acetate as eluant. A violet band separated, which was extracted with methanol (Yield: 0.013 g, 0.024 mmol, 80%).

2.3.6.1. Procedure (2). The ligand HL^6 (0.071 g, 0.24 mmol) was reacted with the salt $K_2[PtCl_4]$ (0.1 g, 0.24 mmol) in boiling aqueous acetonitrile (CH_3CN: H_2O, 9: 1) to produce Complex $[PdL^6Cl]$ in excellent yields (89%). Procedure was same as described earlier.

Anal. Calc. for $C_{17}H_{13}N_2OSClPt$: C, 39; H, 2.5; N, 5.3. Found: C, 38.6; H, 2.2; N, 5.0%. IR (KBr; ν/cm^{-1}): 1438 (–N=N–). UV–Vis (CH_2Cl_2), λ/nm ($\varepsilon/dm^3\,mol^{-1}\,cm^{-1}$): 306 (7700), 376 (4100), 528 (4000), 566 (5300). ^{1}H NMR in $CDCl_3$ (ppm): 3.02 (s, 3H, $-SCH_3$), 7.26 (m, 2H), 7.47–7.49 (m, 4H), 7.71–7.74 (m, 2H), 8.46 (d, 1H, J = 8.2 Hz), 8.82 (d, 1H, J = 8.4 Hz). MS: m/z 523 $[M]^+$.

2.3.7. Isolation of $[Pt(L^7)Cl]$ (**7**)

$[Pt(L^7)Cl]$ (**7**) was made following the same procedure of complex **6**. The following yield is based on HL^7 (0.009 g, 0.03 mmol) and $[Pt(allyl)Cl]_2$ (0.009 g, 0.015 mmol) (Yield: 0.013 g, 0.024 mmol, 79%). *Anal.* Calc. for $C_{18}H_{15}N_2OSClPt$: C, 40; H, 2.8; N, 5.2. Found: C, 38.6; H, 2.6; N, 4.8%. IR (KBr; ν/cm^{-1}): 1436 (–N=N–). UV–Vis (CH_2Cl_2), λ/nm ($\varepsilon/dm^3\,mol^{-1}\,cm^{-1}$): 307 (8300), 374 (4500), 528 (4300), 564 (5500). ^{1}H NMR in $CDCl_3$ (ppm): 3.47 (m, 2H, $-SCH_2$), 1.21 (t, 3H, $-CH_3$), 7.18–7.78 (m, 8H, complex pattern), 8.56 (d, 1H), 8.78 (d, 1H). MS: m/z 537 $[M]^+$.

2.3.8. Isolation of $[Pt(L^8)Cl]$ (**8**)

$[Pt(L^8)Cl]$ (**8**) was made following the same procedure of complex **6**. The amount of HL^8 and $[Pt(allyl)Cl]_2$ complex used were (0.01 g, 0.03 mmol) and (0.01 g, 0.015 mmol) respectively.

(Yield: 0.012 g, 0.023 mmol, 75%). *Anal.* Calc. for $C_{19}H_{17}N_2OSClPt$: C, 41.3; H, 3.1; N, 5.1. Found: C, 40.8; H, 2.8; N, 4.8%. IR (KBr; ν/cm^{-1}): 1439 (–N=N–). UV–Vis (CH_2Cl_2), λ/nm ($\varepsilon/dm^3\,mol^{-1}\,cm^{-1}$): 301 (9700)(9(9700),700), 369 (5300), 531 (4400), 564 (5600). ^1H NMR in $CDCl_3$ (ppm): 3.46 (m, 2H, $-SCH_2$), 1.24 (m, 2H, $-CH_2$), 1.04 (t, 3H, $-CH_3$), 7.18 (t, 1H), 7.40–7.53 (m, 5H), 7.75–7.85 (m, 2H), 8.11 (d, 1H, J = 8.2 Hz), 8.78 (d, 1H, J = 8.4 Hz). MS: m/z 551 $[M]^+$.

2.3.9. Isolation of [Pt(L^9)Cl] (**9**)

[Pt(L^9)Cl] (**9**) was made following the same procedure of complex **6**. The amount of HL^9 and [Pt(allyl)Cl]$_2$ used were (0.01 g, 0.03 mmol) and (0.009 g, 0.015 mmol) respectively. (Yield: 0.014 g, 0.024 mmol, 80%). *Anal.* Calc. for $C_{20}H_{19}N_2OSClPt$: C, 42.4; H, 3.4; N, 5. Found: C, 41.9; H, 3.0; N, 4.7%. IR (KBr; ν/cm^{-1}): 1437 (–N=N–). UV–Vis (CH_2Cl_2), λ/nm ($\varepsilon/dm^3\,mol^{-1}\,cm^{-1}$): 307 (9000), 374 (5000), 528 (4500), 565 (5800); ^1H NMR in $CDCl_3$ (ppm): 3.47 (m, 2H, $-SCH_2$), 1.61 (m, 2H, $-CH_2$), 1.21 (m, 2H, $-CH_2$), 0.86 (m, 3H, $-CH_3$), 7.15–7.80 (m, 8H, complex pattern), 8.56 (d, 1H), 8.86 (d, 1H). MS: m/z 565 $[M]^+$.

2.3.10. Isolation of [Pt(L^{10})Cl] (**10**)

The preparation of [Pt(L^{10})Cl] (**10**) was made following the above procedure. The following yield is based on HL^{10} (0.011 g, 0.03 mmol) and [Pt(allyl)Cl]$_2$ (0.009 g, 0.015 mmol). (Yield: 0.012 g, 0.02 mmol, 65%). *Anal.* Calc. for $C_{23}H_{17}N_2OSClPt$: C, 46; H, 2.8; N, 4.7. Found: C, 45.6; H, 2.68; N, 4.1%. IR (KBr; ν/cm^{-1}): 1436 (N=N). UV–Vis (CH_2Cl_2), λ/nm ($\varepsilon/dm^3\,mol^{-1}\,cm^{-1}$): 307(10200), 375(6400), 533(5300), 565(6500); ^1H NMR in $CDCl_3$ (ppm): 3.48 (m, 2H, $-SCH_2$), 6.82 (d, 1H, J = 8.2 Hz), 7.12–7.56 (m, 6H), 7.41–7.59 (m, 4H), 8.20 (br, 2H), 8.87 (d, 1H, J = 7.8 Hz). MS: m/z 599 $[M]^+$.

2.4. Preparation of the iodo-compounds

2.4.1. Isolation of [Pt(L^1)I] (**11**)

A dichloromethane solution containing iodine (1%) was added drop wise to a pink colored dichloromethane solution (10 mL) of [Pt(L^1)Cl] (**1**) (0.018 g, 0.035 mmol) with stirring till the pink color of the reaction mixture changed to pinkish violet. The mixture was chromatographed on TLC and a violet band containing [Pt(L^1)I] was eluted by benzene. Shining crystals of (**11**) were collected by evaporation of the solvent. (Yield: 80%). *Anal.* Calc. for $C_{17}H_{13}N_2OSIPt$: C, 33.2; H, 2.1; N, 4.6. Found: C, 33; H, 1.8; N, 4.1%. IR (KBr; ν/cm^{-1}): 1436 (–N=N–). UV–Vis (CH_2Cl_2), λ/nm ($\varepsilon/dm^3\,mol^{-1}\,cm^{-1}$): 308 (6000), 408 (7200), 526 (5400), 560 (7500). ^1H NMR in $CDCl_3$ (ppm): 3.0 (s, 3H, $-SCH_3$), 7.35–7.46 (m, 4H), 7.56 (br, 2H), 7.72 (m, 2H), 8.62-8.67 (m, 2H). MS: m/z 615 $[M]^+$.

2.4.2. Isolation of [Pt(L^2)I] (**12**)

This compound was synthesized following method described above. Amount of [Pt(L^2)Cl] used was (0.019 g, 0.035 mmol). (Yield: 76%). *Anal.* Calc. for $C_{18}H_{15}N_2OSIPt$: C, 34.3; H, 2.4; N, 4.5. Found: C, 34; H, 2.1; N, 4.2%. IR (KBr; ν/cm^{-1}): 1438 (–N=N–). UV–Vis (CH_2Cl_2), λ/nm ($\varepsilon/dm^3\,mol^{-1}\,cm^{-1}$): 309 (7400), 409 (7900), 527 (5700), 562 (7900). ^1H NMR in $CDCl_3$ (ppm): 3.48 (m, 2H, $-SCH_2$), 1.21 (t, 3H, $-CH_3$), 7.36–8.66 (aromatic protons). MS: m/z 629 $[M]^+$.

2.4.3. Isolation of [Pt(L^3)I] (**13**)

This complex was prepared in the same process as mentioned above. The following yield is based on [Pt(L^3)Cl] (0.011 g, 0.02 mmol). (Yield: 76%). *Anal.* Calc. for $C_{19}H_{17}N_2OSIPt$: C, 35.5; H, 2.6; N, 4.4. Found: C, 35.1; H, 2.2; N, 4.1%. IR (KBr; ν/cm^{-1}): 1437 (–N=N–). UV–Vis (CH_2Cl_2), λ/nm ($\varepsilon/dm^3\,mol^{-1}\,cm^{-1}$): 310 (7400), 410 (9800), 528 (6900), 564 (10000). ^1H NMR in $CDCl_3$ (ppm): 3.47 (m, 2H, $-SCH_2$), 1.24 (m, 2H, $-CH_2$), 1.01 (t, 3H, $-CH_3$), 7.30-8.90 (aromatic protons). MS: m/z 643 $[M]^+$.

2.4.4. Isolation of [Pt(L^4)I] (**14**)

This compound was sysnthesized following method described above. The following yield is based on [Pt(L^4)Cl] (0.023 g, 0.04 mmol). (Yield: 78%). *Anal.* Calc. for $C_{20}H_{19}N_2OSIPt$: C, 36.5; H, 2.9; N, 4.3%. Found: C, 36.2; H, 2.5; N, 4.1%. IR (KBr; ν/cm^{-1}): 1436 (–N=N–). UV–Vis (CH_2Cl_2), λ/nm ($\varepsilon/dm^3\,mol^{-1}\,cm^{-1}$): 310 (8000), 410 (10300), 527 (7100), 564 (10300). ^1H NMR in $CDCl_3$ (ppm): 3.48 (m, 2H, $-SCH_2$), 1.59 (m, 2H, $-CH_2$), 1.21 (m, 2H, $-CH_2$), 0.90 (m, 3H, $-CH_3$), 7.37–7.45 (m, 5H), 7.58 (br, 2H), 7.71 (br, 2H), 8.64 (m, 1H). MS: m/z 657 $[M]^+$.

2.4.5. Isolation of [Pt(L^5)I] (**15**)

The preparation of [Pt(L^5)I] (**15**) was made following the above procedure. Amount of [PtL^5Cl] used was (0.023 g, 0.038 mmol). (Yield: 79%). *Anal.* Calc. for $C_{23}H_{17}N_2OSIPt$: C, 40; H, 2.5; N, 4.1. Found: C, 39.8; H, 2.1; N, 3.8%. IR (KBr; ν/cm^{-1}): 1438 (–N=N–). UV–Vis (CH_2Cl_2), λ/nm ($\varepsilon/dm^3\,mol^{-1}\,cm^{-1}$): 310 (9100), 410 (11000), 527 (7400), 562 (10800). ^1H NMR in $CDCl_3$ (ppm): 3.45 (m, 2H, $-SCH_2$), 7.14–7.26 (m, 6H), 7.29–7.54 (m, 4H), 7.70 (m, 1H), 8.02 (d, 1H, J = 9.3 Hz), 8.49 (d, 1H, J = 8.4 Hz), 8.60 (d, 1H, 8.4 Hz). MS: m/z 691 $[M]^+$.

2.4.6. Isolation of [PtL^6I] (**16**)

A dichloromethane solution containing iodine (1%) was added dropwise to a violet colored solution (10 mL) of [Pt(L^6)Cl] (0.008 g, 0.015 mmol) in CH_2Cl_2 with stirring. Stirring was continued for 2 h till the violet color of the reaction mixture changed to deep violet. The solvent was then evaporated to give a solid mass, which was then chromatographed by TLC using ethyl acetate as eluant. A deep violet band separated, which was then extracted with methanol. (Yield: 82%). *Anal.* Calc. for $C_{17}H_{13}N_2OSIPt$: C, 33.2; H, 2.1; N, 4.6. Found: C, 33.1; H, 1.9; N, 4.2%. IR (KBr; ν/cm^{-1}): 1436 (–N=N–). UV–Vis (CH_2Cl_2), λ/nm ($\varepsilon/dm^3\,mol^{-1}\,cm^{-1}$): 314 (12600), 390 (6500), 538 (4600), 576 (5800). ^1H NMR in $CDCl_3$ (ppm): 3.01 (s, 3H, $-SCH_3$), 7.19–7.77 (8H), 8.53 (d, 1H, J = 8.1 Hz), 8.81 (d, 1H, J = 8.4 Hz). MS: m/z 615 $[M]^+$.

2.4.7. Isolation of [Pt(L^7)I] (**17**)

This compound was synthesized following method described above. The following yield is based on [Pt(L^7)Cl] (0.008 g, 0.015 mmol).

(Yield: 80%). *Anal.* Calc. for $C_{18}H_{15}N_2OSIPt$: C, 34.3; H, 2.4; N, 4.5. Found: C, 34.1; H, 2; N, 4.1%. IR (KBr; ν/cm^{-1}): 1437 (–N=N–). UV–Vis (CH_2Cl_2), λ/nm ($\varepsilon/dm^3\,mol^{-1}\,cm^{-1}$): 312 (10400), 390 (5800), 538 (4800), 574 (6200). ^1H NMR in $CDCl_3$ (ppm): 3.46 (m, 2H, $-SCH_2$), 1.19 (t, 3H, $-CH_3$), 7.19–8.68 (aromatic protons). MS: m/z 629 $[M]^+$.

2.4.8. Isolation of [Pt(L^8)I] (**18**)

The preparation of [Pt(L^8)I] (**18**) was made following the above procedure. The amount of [Pt(L^8)Cl] (**8**) used was (0.008 g, 0.015 mmol). (Yield: 84%). *Anal.* Calc. for $C_{19}H_{17}N_2OSIPt$: C, 35.5; H, 2.6; N, 4.4. Found: C, 35.2; H, 2.2; N, 4%. IR (KBr; ν/cm^{-1}): 1438 (–N=N–). UV–Vis (CH_2Cl_2), λ/nm ($\varepsilon/dm^3\,mol^{-1}\,cm^{-1}$): 312 (11200), 369 (5700), 538 (5100), 575 (6700). ^1H NMR in $CDCl_3$ (ppm): 3.46 (m, 2H, $-SCH_2$), 1.21 (m, 2H, $-CH_2$), 1.0 (t, 3H, $-CH_3$), 7.18–7.80 (8H), 8.51 (d, 1H, J = 8.2 Hz), 8.84 (d, 1H, J = 8.2 Hz). MS: m/z 643 $[M]^+$.

2.4.9. Isolation of [Pt(L^9)I] (**19**)

The preparation of [Pt(L^9)I] (**19**) was made following the above procedure. The amount of [Pt(L^9)Cl] (**9**) used was (0.009 g, 0.015 mmol). (Yield: 80%). *Anal.* Calc. for $C_{20}H_{19}N_2OSIPt$: C, 36.5; H, 2.9; N, 4.3. Found: C, 36.1; H, 2.6; N, 4%. IR (KBr; ν/cm^{-1}): 1436 (–N=N–). UV–Vis (CH_2Cl_2), λ/nm ($\varepsilon/dm^3\,mol^{-1}\,cm^{-1}$): 312 (12300), 368 (6400), 538 (5500), 575 (7000). ^1H NMR in $CDCl_3$

(ppm): 3.45 (m, 2H,–SCH_2), 1.51 (m, 2H,–CH_2), 1.18 (m, 2H,–CH_2), 0.90 (m, 3H, –CH_3), 7.19–7.70 (8H), 8.54 (m, 1H), 8.81 (d, 1H, J = 8.4 Hz). MS: m/z 657 $[M]^+$.

2.4.10. Isolation of [Pt(L^{10}) I] (**20**)

The compound [Pt(L^{10})I] (**20**) was synthesized following the described method. The following yield is based on [Pt(L^{10})Cl] (**10**) (0.009 g, 0.015 mmol). (Yield: 85%). *Anal.* Calc. for $C_{23}H_{17}N_2OSIPt$: C, 40; H, 2.5; N, 4.1. Found: C, 39.8; H, 2.2; N, 3.9%. IR (KBr; ν/cm^{-1}): 1438 (–N=N–). UV–Vis (CH_2Cl_2), λ/nm (ε/dm^3 mol^{-1} cm^{-1}): 312 (14500), 369 (7100), 538 (6200), 575 (8100). ^{1}H NMR in $CDCl_3$ (ppm): 3.41 (m, 2H, –SCH_2), 7.18–7.77 (8H), 8.51 (d, 1H, J = 8.0 Hz), 8.82 (d, 1H, J = 8.3 Hz). MS: m/z 691 $[M]^+$.

2.5. Physical measurements

C, H and N elemental analyses were done by either Perkin-Elmer (Model 240C) or Heraeus Carlo Ebra 1108 elemental analyzer. The IR spectra were obtained on Jasco 5300 FT-IR. Visible and ultraviolet spectra were recorded on a Jasco V-530 spectrophotometer. ^{1}H NMR spectra were measured in $CDCl_3$ with a Bruker Avance DPX 300 spectrophotometer with $SiMe_4$ as an internal standard. The FAB mass spectra were recorded on a JEOL SX 102/DA-6000 Mass Spectrometer/Data System using Argon/Xenon (6 kV, 10 mA) as the FAB gas. ESI mass spectra were recorded on a Micromass Quattro II triple quadrupole mass spectrometer.

2.6. Crystallography

Single crystals of (**3**), (**9**) and (**13**) were grown by slow diffusion of n-hexane into the dichloromethane solution of the complexes. A suitable single crystal was carefully selected under a polarizing microscope and glued to a thin glass fiber with cynaoacrylate adhesive. Selected crystal data and data collection parameters are given in Table 1. Crystallographic data collections were performed on a Bruker SMART 1000 CCD area-detector diffractometer using graphite monochromated Mo Kα (λ = 0.71073 Å) radiation by ω scan. The structure was solved by direct methods using SHELXS-97 [31] and difference Fourier syntheses and refined with SHELXL97 package incorporated in WINGX 1.64 crystallographic collective package [32]. All the hydrogen positions for the compound were initially located in the difference Fourier map, and for the final refinement, the hydrogen atoms were placed geometrically and held in the riding mode. The last cycles of refinement included atomic positions for all the atoms, anisotropic thermal parameters for all non-hydrogen atoms and isotropic thermal parameters for all the hydrogen atoms. Full-matrix-least-squares structure refinement against $|F^2|$. Molecular geometry calculations were performed with PLATON [33], and molecular graphics were prepared using ORTEP-3 [34].

2.7. Method and computational details

The calculations have been performed within the TD-DFT formalism as implemented in ADF2007 [35]. Two approximations are generally made: one for the XC potential, and one for the XC kernel, which is the functional derivative of the time-dependent XC potential with respect to density. We used LDA (local density approximation) including the VWN parametrization [36] in the SCF step and Becke [37] and Perdew–Wang [38] gradient corrections to the exchange and correlation respectively and Adiabatic local Density Approximation (ALDA) for the XC kernel, in the post-SCF step. TD-DFT calculations have been performed with the uncontracted triple-STO basis set with a polarization function for

Table 1
Crystal data and structure refinement table for the platinum(II) complexes.

	[Pt(L^3)Cl] (**3**)	[Pt(L^9)Cl] (**9**)	[Pd(L^3)I] (**13**)
CCDC Deposition Number	869984	876267	869985
Empirical formula	$C_{19}H_{17}ClN_2OPtS$	$C_{20}H_{19}ClN_2OPtS$	$C_{19}H_{17}IN_2OPtS$
Formula weight	551.95	565.97	643.40
T (K)	293(2)	293(2)	293(2)
λ (Å)	0.71073	0.71073	0.71073
Crystal system	monoclinic	monoclinic	monoclinic
Space group	$P21/n$	$P21/n$	$P21/n$
Unit cell dimensions			
a (Å)	12.2720(4)	11.478(4)	13.531(3)
b (Å)	8.9594(3)	8.913(3)	9.007(18)
c (Å)	8.976(4)	18.736(6)	16.564(3)
α (°)	90	90	90
β (°)	108.213(2)	100.916(4)	108.50(3)
γ (°)	90	90	90
V (Å^3)	1836.61(11)	1836.61(11)	1914.4(7)
Z	4	4	4
D_{calc} (Mg/m^3)	1.996	1.997	2.232
Absorption coefficient (mm^{-1})	7.908	7.720	9.060
F(000)	1056	1088	1200
Crystal size (mm)	0.35 × 0.17 × 0.13	0.37 × 0.21 × 0.11	0.28 × 0.19 × 0.09
θ Range for data collection	1.79–25.00°	1.93–25.00°	3.18–24.99°
Limiting indices	$-13 \leqslant h \leqslant 14$ $-10 \leqslant k \leqslant 10$ $-20 \leqslant l \leqslant 19$	$-13 \leqslant h \leqslant 13$ $-10 \leqslant k \leqslant 10$ $-22 \leqslant l \leqslant 22$	$-7 \leqslant h \leqslant 16$ $-10 \leqslant k \leqslant 10$ $-19 \leqslant l \leqslant 11$
Reflections collected	22771	14037	4151
Independent reflections	3224 [R_{int} = 0.0359]	3319 [R_{int} = 0.0426]	2918 [R_{int} = 0.0970]
Data/restraints/parameters	3224/0/227	3319/0/236	2918/0/227
Goodness-of-fit on F^2	1.064	1.049	0.866
Final R indices [$I > 2\sigma(I)$]	R_1 = 0.0184, wR_2 = 0.0472	R_1 = 0.0279, wR_2 = 0.0668	R_1 = 0.0385, wR_2 = 0.0713
R indices (all data)[a,b]	R_1 = 0.0222, wR_2 = 0.0489	R_1 = 0.0341, wR_2 = 0.0701	R_1 = 0.0541, wR_2 = 0.0751
Largest difference in peak and hole (e Å^{-3})	0.635 and −0.659	2.056 and −0.565	1.381 and −0.708

[a] $R = \Sigma||F_o| - |F_c||/\Sigma|F_o|$.
[b] $Rw = [\Sigma w(|F_o|^2 - |F_c|^2)/\Sigma w(F_o^2)^2]^{1/2}$.

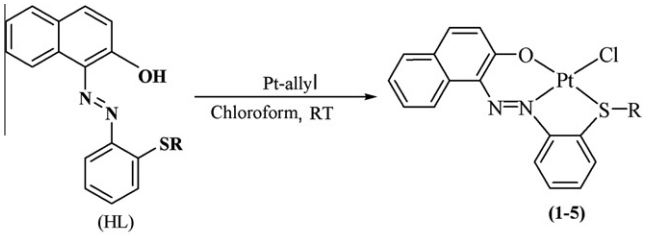

1: R = CH_3; **2**: R = C_2H_5; **3**: R = C_3H_7; **4**: R = C_4H_9; **5**: R = CH_2Ph

Scheme 1. Reactions of $[(\eta^3\text{-}C_4H_7)Pt(\mu\text{-}Cl)]_2$ with the azo-ligands (HL^1–HL^5).

all atoms. In the calculation of the optical spectra, 70 lowest spin-allowed singlet–singlet transitions have been taken into account. Transition energies and oscillator strengths have been interpolated by a Gaussian convolution with a s of 0.2 eV. Solvent effects were modelled by the "Conductor-like Screening Model" (COSMO) [39] of solvation as implemented in ADF.

3. Results and discussion

2-Hydroxy-1-(2′-alkylthiophenylazo)naphthalenes (HL^1–HL^5) slowly react with $[(\eta^3\text{-}C_4H_7)Pt(\mu\text{-}Cl)]_2$ in chloroform at room temperature (reaction time: 24 h) and the color of the reaction mixture turns into pink (Scheme 1). Crystalline pink colored complexes [Pt^{II}LCl] (**1**–**5**) were isolated using thin layer chromatography.

Higher yield of the complexes was achieved following an alternative route. Complexes (**1**–**5**) were obtained by refluxing $K_2[PtCl_4]$ with 2-hydroxy-1-(2′-alkylthiophenylazo) naphthalenes (HL^1–HL^5) in acetonitrile. The reaction time is 3 h and the yield is more than 85%. It is noteworthy that refluxing $K_2[PtCl_4]$ with diazene based ligands in acetonitrile often leads to the formation of platinum(IV) complexes [40]. The formation of exclusive platinum(II) complexes in the present case indicates the softness of the ligand frame.

The structure of complex (**3**) as a representative case has been determined unambiguously by X-ray crystallography. The molecular structure is shown in Fig. 1. The crystal data for the complex **3** and its selected bond parameters are given in Tables 1 and 2, respectively. The structure shows that the crystal lattice of this complex contains discrete molecules. The structure shows that the platinum(II) center is bonded to O1 of the naphtholato function, N2 of the diazene group and S1 at the 2′ position of the phenyl fragment and the fourth coordination position is occupied by a chloride ion. Therefore, 2-hydroxy-1-(2′-alkylthiophenylazo)naphthalene binds platinum(II) as a monoanionic tridentate O,N,S ligand forming a five membered chelate ring and a six-membered chelate ring with bite angles 87.58(8)° (N2–Pt1–S1) and 92.99(10)° (N2–Pt1–O1), respectively. The tetra coordination around platinum is essentially planner, but in a distorted square planner geometry.

The reactivity of another group of terdentate ligands (HL^6–HL^{10}) with O,N,S donor set with platinum(II) was examined. The di-μ-chloro-bis(η^3-2-methylallyl)diplatinum(II) was found to react with 1-hydroxy-2-(2′-alkylthiophenylazo)naphthalenes in chloroform leading to the violet product [Pt^{II}LCl] (**6**–**10**) (Scheme 2).

The molecular structure of complex (**9**) has been determined by X-ray crystallography. The molecular structure is shown in Fig. 2. The crystal data for the complex (**9**) and its selected bond parameters are given in Table 1 and 3, respectively. The structure shows that 1-hydroxy-2-(2′-alkylthiophenyl-azo)naphthalene binds platinum(II) as a monoanionic tridentate (O,N,S) ligand and the fourth coordination position is occupied by a chloride ion. Here also, the reaction of tridentate diazene ligands (HL^6–HL^{10}) with tetrachloroplatinate(II) in refluxing acetonitrile medium affords platinum(II) complexes in higher yield.

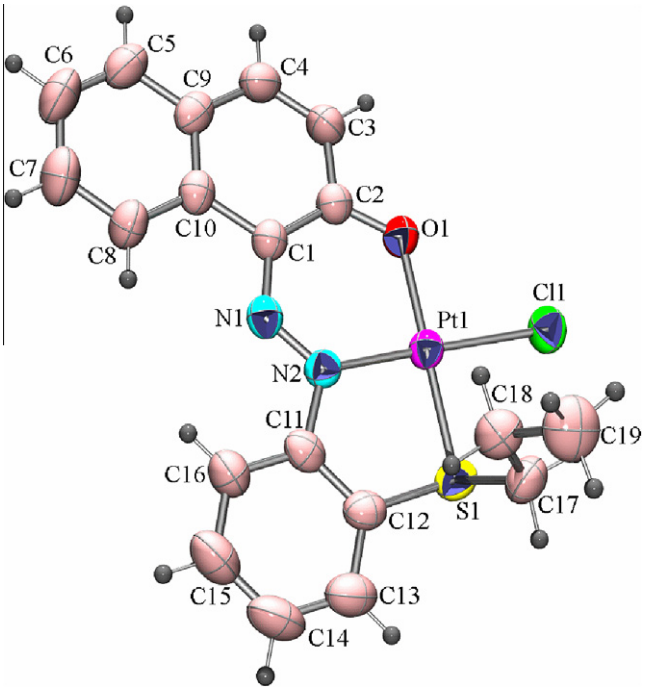

Fig. 1. ORTEP drawing of the compound (**3**). Thermal ellipsoids are drawn at 50% probability.

Table 2
Selected bond lengths (Å) and bond angles (°) for the complex (**3**).

	Bond lengths (Å)		Bond angles (°)
Pt(1)–N(2)	1.954(3)	N(2)–Pt(1)–O(1)	92.99(10)
Pt(1)–O(1)	1.993(2)	N(2)–Pt(1)–S(1)	87.58(8)
Pt(1)–S(1)	2.2266(10)	O(1)–Pt(1)–S(1)	178.54(7)
Pt(1)–Cl(1)	2.3194(9)	N(2)–Pt(1)–Cl(1)	177.95(8)
N(1)–N(2)	1.293(4)	O(1)–Pt(1)–Cl(1)	88.49(7)
N(1)–C(1)	1.350(4)	S(1)–Pt(1)–Cl(1)	90.98(4)
N(2)–C(11)	1.441(4)		

3.1. Reactivity of [PtLCl] complexes with halogens and alkyl halides

Platinum compounds [Pt^{II}(L)Cl] (**1**–**10**) readily undergo reaction with iodine in dichloromethane medium at room temperature (300 K) (Scheme 3). The product [Pt^{II}(L)I] was isolated by thin layer chromatography on silica gel plate using 10% CH_3COOEt in petroleum ether as eluant. The reaction of [Pt^{II}(L)Cl] with alkyl iodide (RI) produces identical product.

X-ray crystallographic analysis of the representative complex (**13**) has been done. The ORTEP diagram with the atom-numbering scheme is shown in Fig. 3. The crystal data for the complex **13** and its selected bond parameters are given in Tables 1 and 4, respectively. The Pt–N(diazene) distances in the square planar complex (**13**) have been found to be slightly longer than that in complex (**3**). The N–N distance in (**13**) (1.261 Å) is shorter than that in complex (**3**) (1.293 Å). The Pt–I distance (2.6007 Å) is comparable to the values reported in the literature [41].

The reactivity pattern of [Pt^{II}(L)Cl] closely resembles the previously reported systems [41].

The following sequences seem reasonable: (a) initial formation of an octahedral Pt (IV) intermediate with two iodine sitting *trans* to each other, (b) conversion of the *trans* isomer to thermodynamically

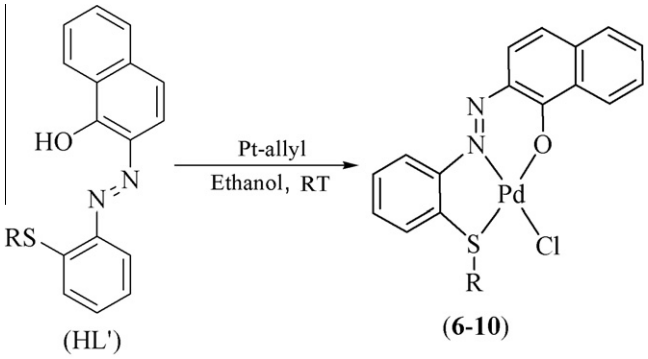

6: R = CH_3; **7**: R = C_2H_5; **8**: R = C_3H_7; **9**: R = C_4H_9; **10**: R = CH_2Ph

Scheme 2. Reactions of $[(\eta^3\text{-}C_4H_7)Pt(\mu\text{-}Cl)]_2$ with the azo-ligands (HL^6–HL^{10}).

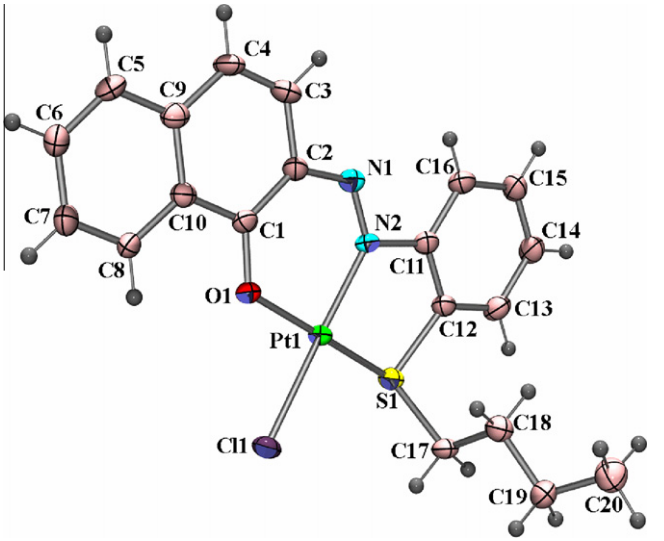

Fig. 2. ORTEP drawing of the compound (**9**). Thermal ellipsoids are drawn at 50% probability.

Table 3
Selected bond lengths (Å) and bond angles (°) for the complex (**9**).

	Bond lengths (Å)		Bond angles (°)
Pt(1)–N(2)	1.968(4)	N(2)–Pt(1)–O(1)	92.94(15)
Pt(1)–O(1)	2.003(3)	N(2)–Pt(1)–S(1)	87.29(12)
Pt(1)–S(1)	2.2241(13)	O(1)–Pt(1)–S(1)	176.50(10)
Pt(1)–Cl(1)	2.3200(15)	N(2)–Pt(1)–Cl(1)	178.40(12)
N(1)–N(2)	1.281(5)	O(1)–Pt(1)–Cl(1)	88.55(10)
N(1)–C(2)	1.355(6)	S(1)–Pt(1)–Cl(1)	91.25(5)
N(2)–C(11)	1.448(6)		

more stable *cis* form, (c) dissociation of Cl^- giving the five coordinate intermediate and finally (d) reductive elimination of I–Cl leading to the formation of $[Pt^{II}(L)I]$.

3.2. UV–Vis spectra and excited singlet state calculations

All the platinum(II) complexes are soluble in common organic solvents such as dichloromethane, acetonitrile, acetone, etc., producing intense violet solutions. Spectral data are presented in the Experimental Section. Electronic spectral patterns of the platinum(II) complexes have been shown in Fig. 4.

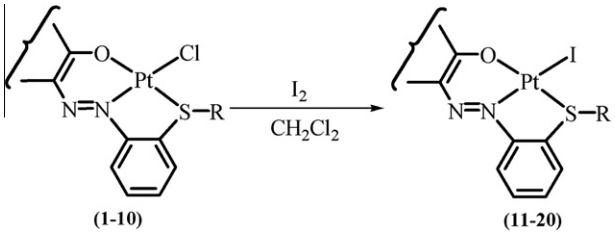

Scheme 3. Reactions of platinum(II) complexes (**1**–**10**) with iodine at room temperature.

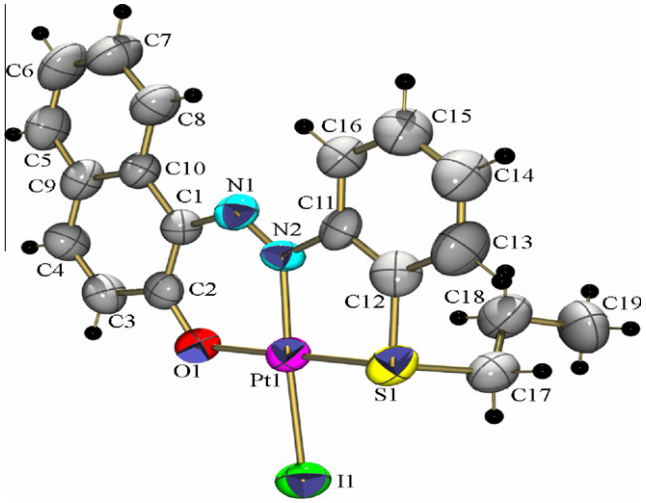

Fig. 3. ORTEP diagram of the platinum(II) compound (**13**). Thermal ellipsoids are drawn at 50% probability.

Table 4
Selected bond lengths (Å) and bond angles (°) for the complex (**13**).

	Bond lengths (Å)		Bond angles (°)
Pt(1)–N(2)	1.980(6)	N(2)–Pt(1)–O(1)	92.4(2)
Pt(1)–O(1)	2.003(5)	N(2)–Pt(1)–S(1)	87.17(18)
Pt(1)–S(1)	2.222(2)	O(1)–Pt(1)–S(1)	177.76(16)
Pt(1)–I(1)	2.6007(8)	N(2)–Pt(1)–I(1)	176.97(18)
N(1)–N(2)	1.261(8)	O(1)–Pt(1)–I(1)	89.03(15)
N(1)–C(1)	1.369(9)	S(1)–Pt(1)–I(1)	91.54(6)
N(2)–C(11)	1.429(10)		

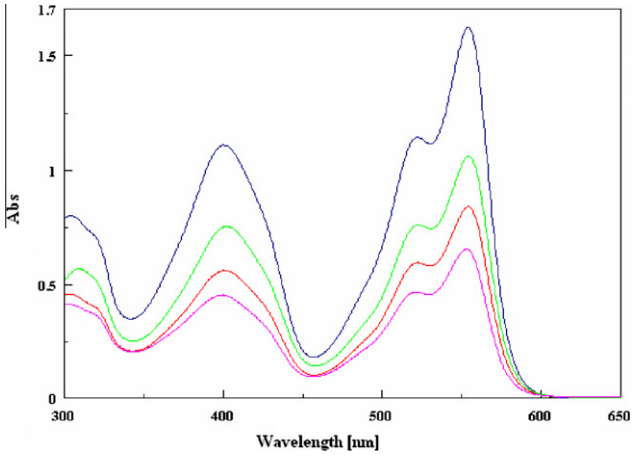

Fig. 4. Electronic spectra of (**1**) (pink), (**3**) (blue), (**4**) (red) and (**5**) (green). (For interpretation of the references to color in this figure legend, the reader is referred to the web version of this article.)

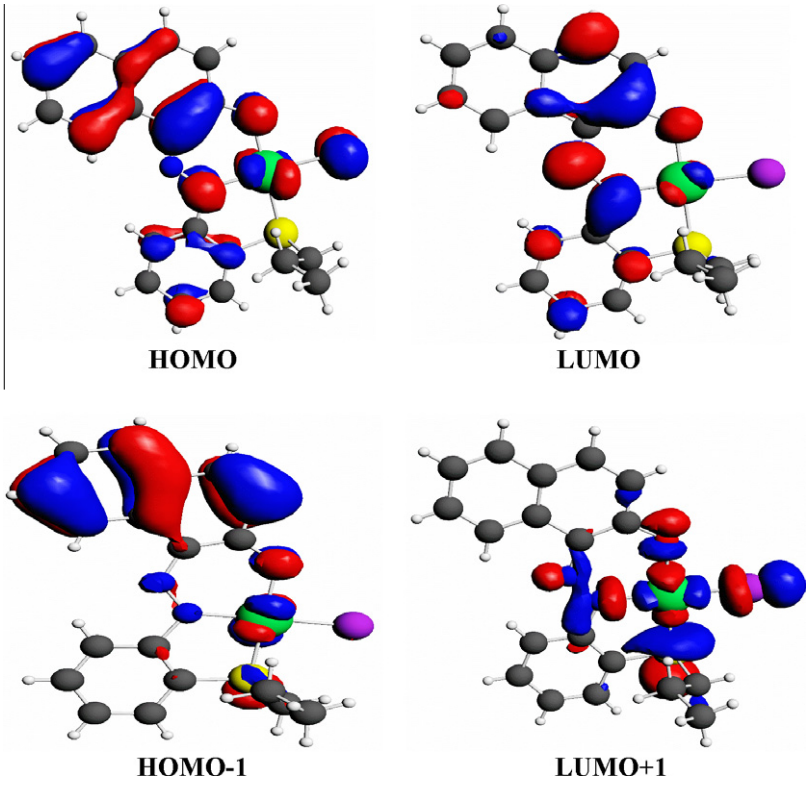

Fig. 5. Selected FMO's of the complex (**3**).

TD-DFT calculation was carried out on the representative platinum(II) complexes (**3**, **9** and **13**) to gain insight into the electronic features of these complexes and also to understand the nature of the low-lying excitation states.

All the platinum(II) complexes have been found to have similar molecular orbitals. The relative contributions of each moiety to the corresponding MOs are listed in the Supplementary information (Table S1–S3). Selected FMOs for the complex **3** are shown in Fig. 5. The calculations show that the HOMOs of all the three complexes (**3**, **9** and **13**) are mostly concentrated on the diazene ligand, with very little contribution from the d(Pt) orbitals. For the complex **3**, HOMO−1 and HOMO−2 are also based primarily on the ligand framework. Whereas, in HOMO−3 and HOMO−4, substantial amount of d(Pt) (22% and 44%, respectively) contribution has been noted. Apart from LUMO+1, which has a contribution of 39% metal character, all other unoccupied MOs are ligand based. On the other hand, HOMO−2, HOMO−3 and HOMO−4 contain sizeable contribution from the d(Pt) orbitals (21%, 30% and 40% respectively). For, the platinum(II) complex (**13**), in contrast the HOMO is largely ligand based. However, HOMO−1 is largely concentrated on the terminal iodido ligand. Significant amount of contributions from d(Pt) orbitals arise in HOMO−4 and HOMO−5 orbitals.

The excitation energies (eV), wavelengths (nm), oscillator strengths (eV) and dominating contributing configurations obtained at the TD-DFT/PW91/TZP level of theory for complexes (**3**, **9** and **13**) are provided in Tables S4–S6. The calculations show that electronic transition with dominant contributing configurations involving the HOMO → LUMO orbital pair occur at 551 nm (1st excited state for **3**), 582 nm (1st excited state for **9**) and 594 nm (1st excited state for **13**). The value obtained agrees well with the observed bands, suggesting the suitability of the calculations for these complexes. According to TD-DFT, these low-energy transitions are indicative of intraligand charge transfer (ILCT) transition having a small admixture of MLCT transitions. The other absorptions in the visible region in have common density redistribution features with a significant amount of metal to ligand charge transfer and more or less π–π^* intraligand density redistribution (Tables S4–S6).

4. Conclusions

2-Hydroxy-1-(2′-alkylthiophenylazo)naphthalenes (HL^1–HL^5) and 1-hydroxy-2-(2′-alkylthiopheny-lazo)naphthalenes (HL^6–HL^{10}) smoothly form planar platinum(II) complexes through O,N,S donor set. Tetra coordination around platinum is essentially planner, but in a distorted square planner geometry having six-membered Pt(1)–O(1)–C(1)–C(2)–N(1)–N(2) chelate ring and five-membered Pt(1)–N(2)–C(11)–C(12)–S(1) chelate rings. Compounds [Pt^{II}(L)Cl] react with iodine and afford complexes [Pt^{II}(L)I]. The simulated electronic spectra of the platinum(II) complexes using time-dependent density functional theory (TD-DFT) are in close agreement with the experimental spectra. The low energy absorptions are attributed to intraligand charge transfer transitions having admixtures of metal-to-ligand charge-transfer transitions whereas the high energy absorptions are due to ILCT and LLCT transitions.

Acknowledgments

The financial support from the SERB, Department of Science & Technology (SR/S1/IC-53/2010) and CSIR (1/2498/11/EMR-II), New Delhi are gratefully acknowledged. We also thank CSIR for the award of fellowship to A.K.

Appendix A. Supplementary material

CCDC 869984, 869985 and 8762687 contains the supplementary crystallographic data for this paper. These data can be obtained free of charge from The Cambridge Crystallographic Data

Centre via http://www.ccdc.cam.ac.uk/data_request/cif. Supplementary data associated with this article can be found, in the online version, at http://dx.doi.org/10.1016/j.ica.2012.09.041.

References

[1] V. Rosenberg, L. van Camp, T. Krigas, Nature 205 (1965) 698.
[2] R. Bakhtiar, E.I. Ochiai, Gen. Pharm. 32 (1999) 525.
[3] N. Farrell, Coord. Chem. Rev. 232 (2002) 1.
[4] (a) J. Dupont, C.S. Consorti, J. Spencer, Chem. Rev. 105 (2005) 2527;
(b) M.E. van der Boom, D. Milstein, Chem. Rev. 103 (2003) 1759;
(c) A.D. Ryabov, Chem. Rev. 90 (1990) 403.
[5] L.J. Teixeira, M. Seabra, E. Reis, M.T. Girão da Cruz, M.C. Pedroso de Lima, E. Pereira, M.A. Miranda, M.P.M. Marques, J. Med. Chem. 47 (2004) 2917.
[6] S.M. Fiuza, A.M. Amado, P.J. Oliveira, V.A. Sardão, L.A.E. Batista de Carvalho, M.P.M. Marques, Lett. Drug Des. Discov. 3 (2006) 149.
[7] A.S. Soares, S.M. Fiúza, M.J. Gonçalves, L.A.E. Batista de Carvalho, M.P.M. Marques, A.M. Urbano, Lett. Drug Des. Discov. 4 (2007) 460.
[8] B. Moriarity, O. Nováková, N. Farrell, V. Brabec, J. Kašpárková, Arch. Biochem. Biophys. 459 (2007) 264.
[9] R.D. Hubbard, S. Fidanze, Comp. Med. Chem. II (7) (2007) 129.
[10] A.S. Abu-Surrah, H.H. Al-Sadoni, M.Y. Abdalla, Cancer Ther. 6 (2008) 1.
[11] N.J. Wheate, J.G. Collins, Curr. Med. Chem. Anticancer Agents 5 (2005) 267.
[12] (a) S.D. Cummings, R. Eisenberg, Inorg. Chem. 34 (1995) 2007;
(b) C. Makedonas, C.A. Mitsopoulou, J. Inorg. Biochem. 86 (2001) 326;
(c) C. Makedonas, C.A. Mitsopoulou, F.J. Lahoz, A.I. Balana, Inorg. Chem. 42 (2003) (2003) 8853.
[13] C. Makedonas, C.A. Mitsopoulou, Eur. J. Inorg. Chem. 3 (2006) 590.
[14] A. Pasini, G.D. Alfons, C. Manzotti, M. Moret, S. Spinelli, M. Valsecchi, Inorg. Chem. 33 (1994) 4140.
[15] G. Faraglia, S. Sitran, D. Montagner, Inorg. Chim. Acta 358 (2005) 971.
[16] C. Metcalfe, J.A. Thomas, Chem. Soc. Rev. 32 (2003) 215.
[17] E. Gao, M. Zhu, H. Yin, L. Liu, Q. Wu, Y. Sun, J. Inorg. Biochem. 102 (2008) 1958.
[18] T. Rau, R. Alsfasser, A. Zahl, R. van Eldik, Inorg. Chem. 37 (1998) 4223.
[19] (a) P.P. Corbi, F. Cagnin, L.P.B. Sabeh, A.C. Massabni, C.M. Costa-Neto, Spectrochim. Acta, Part A 66 (2007) 1171;
(b) P.P. Corbi, A.C. Massabni, L.P.B. Sabeh, C.M. Costa-Neto, J. Coord. Chem. 61 (2008) 2470.
[20] A. Garza-Ortiz, H. den Dulk, J. Brouwer, H. Kooijman, A.L. Spek, J. Reedijk, J. Inorg. Biochem. 101 (2007) 1922.
[21] S. Chattopadhyay, C. Sinha, P. Basu, A. Chakravorty, Organometallics 10 (1991) 1135.
[22] S. Chattopadhyay, C. Sinha, P. Basu, A. Chakravorty, J. Organomet. Chem. 414 (1991) 421.
[23] D. Bandyopadhyay, P. Bandyopadhyay, A. Chakravorty, F.A. Cotton, L.R. Falvello, Inorg. Chem. 22 (1983) 1315.
[24] D. Bandyopadhyay, P. Bandyopadhyay, A. Chakravorty, F.A. Cotton, L.R. Falvello, Inorg. Chem. 23 (1984) 1785.
[25] A.N. Biswas, P. Das, V. Bagchi, A. Choudhury, P. Bandyopadhyay, Eur. J. Inorg. Chem. (2011) 3739.
[26] (a) M. Albrecht, Chem. Rev. 110 (2010) 576;
(b) G. Dyker, Angew. Chem., Int. Ed. 38 (1999) 1699;
(c) Y. Guari, S. Sabo-Etienne, B. Chaudret, Eur. J. Inorg. Chem. (1999) 1047;
(d) V. Ritleng, C. Sirlin, M. Pfeffer, Chem. Rev. 102 (2002) 1731;
(e) B.A. Arndtsen, R.G. Bergman, T.A. Mobley, T.H. Peterson, Acc. Chem. Res. 28 (1995) 154.
[27] S. Nandi, D. Banerjee, P. Dutta, T.-H. Lu, A.M.Z. Slawin, C. Sinha, Polyhedron 28 (2009) 3519.
[28] M. Panda, S. Das, G. Mostafa, A. Castiñeiras, S. Goswami, Dalton Trans. (2005) 1249.
[29] M. Ghedini, D. Pucci, A. Crispini, G. Barberio, Organometallics 18 (1999) 2116.
[30] S. Acharya, A. Kejriwal, A.N. Biswas, P. Das, D.N. Neogi, P. Bandyopadhyay, Polyhedron 38 (2012) 50.
[31] G.M. Sheldrick, SHELX97, University of Göttingen, Göttingen, Germany, 1997.
[32] L.J. Farrugia, WINGX Version 1.64, An Integrated System of Windows Programs for the Solution, Refinement and Analysis of Single-Crystal X-ray Diffraction Data, Department of Chemistry, University of Glasgow, 2003.
[33] PLATON: A.L. Spek, J. Appl. Crystallogr. 36 (2003) 7.
[34] L.J. Farrugia, J. Appl. Crystallogr. 30 (1997) 565.
[35] The ADF program system was obtained from Scientific Computing and Modeling, Amsterdam (http://www.scm.com/). For a description of the methods used in ADF, see: G.T. Velde, F.M. Bickelhaupt, E.J. Baerends, C.F. Guerra, S.J.A. Van Gisbergen, J.G. Snijders, T. Ziegler, J. Comput. Chem. 22 (2001) 931.
[36] S.H. Vosco, L. Wilk, M. Nusair, Can. J. Phys. 58 (1980) 1200.
[37] A.D. Becke, Phys. Rev. A38 (1988) 3098.
[38] J.P. Perdew, Y. Wang, Phys. Rev. B45 (1992) 13244.
[39] (a) A. Klamt, G.J. Schüürmann, J. Chem. Soc., Perkin Trans. 2 (1993) 799;
(b) A. Klamt, V. Jonas, J. Chem. Phys. 105 (1996). 9972-3100.
[40] B. Shee, J. Pratihar, S. Chattopadhyay, Polyhedron 25 (2006) 2513.
[41] A. Yahav-Levi, I. Goldberg, A. Vigalok, J. Am. Chem. Soc. 128 (2006) 8710.